LBL--30582

DE91 012860

THE ADVANCED LIGHT SOURCE: A NEW TOOL FOR RESEARCH IN ATOMIC AND MOLECULAR PHYSICS *

Fred Schlachter and Art Robinson

Advanced Light Source
Accelerator and Fusion Research Division
Lawrence Berkeley Laboratory
University of California
Berkeley, CA 94720

April 1991

*This work was supported by the Director, Office of Energy Research, Office of Basic Energy Sciences, Materials Sciences Division of the U.S. Department of Energy, under Contract No. DE-AC03-76SF00098

THE ADVANCED LIGHT SOURCE: A NEW TOOL FOR RESEARCH IN ATOMIC AND MOLECULAR PHYSICS

Fred Schlachter and Art Robinson

Advanced Light Source, Accelerator and Fusion Research Division, Lawrence Berkeley Laboratory, University of California, Berkeley, CA 94720, USA

ABSTRACT

The Advanced Light Source at the Lawrence Berkeley Laboratory will be the world's brightest synchrotron radiation source in the extreme ultraviolet and soft x-ray regions of the spectrum when it begins operation in 1993. It will be available as a national user facility to researchers in a broad range of disciplines, including materials science, atomic and molecular physics, chemistry, biology, imaging, and technology. The high brightness of the ALS will be particularly well suited to high-resolution studies of tenuous targets, such as excited atoms, ions, and clusters.

1. Introduction

Bright, wavelength-tunable light sources make life easier for researchers interested in spectroscopy and scattering experiments. For those working in the ultraviolet or x-ray regions of the spectrum, synchrotron radiation is usually the tool of choice. In fact, the availability of intense, tunable, collimated, polarized radiation has driven the evolutionary development of dedicated facilities optimized for the generation of synchrotron radiation. By 1993, so-called third-generation synchrotron sources will be coming on line in the United States, Europe, and Asia. Next-generation synchrotron light facilities of the type now under construction specialize in producing either soft (long-wavelength) x and ultraviolet radiation (collectively, the XUV) or hard (short-wavelength) x rays by means of insertion devices (undulators and wigglers).

The prospect of exploiting high spectral brightness (flux per unit area of the source, per unit solid angle of the radiation cone, and per unit bandwidth) is the main selling point of the new third-generation synchrotron facilities. The storage rings at these facilities are designed to optimize brightness in two ways. First, the rings contain lengthy straight sections to accommodate long undulators (typically 5 meters in length) with up to 100 or so periods. In general, both photon flux and undulator brightness increase linearly with the number of periods, thereby putting a premium on long undulators with many periods. Second, the rings are designed to have electron (or positron in some cases) beams with a small cross section and a small angular divergence; that is, the storage rings have a small emittance. Since the size and divergence of the electron beam set lower bounds for the radiation-source size and divergence, a low-emittance electron beam translates directly into a high-brightness undulator photon beam. The combination of a very-low-emittance storage ring with optimized undulators makes possible the generation of radiation with a spectral brightness that is a

factor of 20 or more greater than that of existing, second-generation sources, depending on the spectral range. In the past, order-of-magnitude increases in brightness have led to qualitatively new developments in spectroscopic and structural studies of both gas-phase and condensed matter.

Most directly benefiting from high brightness are researchers in both the life and physical sciences who hope to achieve enhanced spatial resolution down to distance scales of about 100 Å in x-ray microscopy and spatially resolved XUV spectroscopy. An example of the latter arises from the study of solid surfaces, which are mostly heterogeneous, making interpretation of spectroscopic data obtained from illuminating the entire surface difficult. With spatial resolution, spectral features could be directly associated with specific surface areas and structures. With existing synchrotron sources, there are a growing number of tantalizing results in x-ray microscopy (including holography) and in spatially resolved x-ray absorption and photoelectron spectroscopy. Moreover, the imaging technology is advancing in step with that of undulators.

For the spectroscopist, the benefits of brightness are substantial but more indirect. Brightness leads to the ability to achieve high spectral resolution without the usual penalty of reduction in signal and increase in measuring time. Experiments with once impracticably long measuring times, perhaps because of inherently weak signals, now become reasonable to contemplate.

Finally, brightness and the naturally pulsed nature of synchrotron radiation bring the ability to observe short-lived or transient systems by means of time-resolved spectroscopic, scattering, and imaging experiments. For example, life scientists hope that, if radiation damage due to the x-ray exposure can be avoided or minimized, it may be possible to image changes in functioning biological cells and cellular structures in near-natural environments. The ultimate time resolution, made possible because there are enough photons in a single pulse of bright synchrotron light to generate a useful signal, would be to follow events in real time on the sub-nanosecond time scale.

Undulators are not invariably the preferred source of synchrotron radiation. For example, the possibility of time-resolved experiments derives more from high photon flux than high brightness. As it happens, undulators tend to generate higher photon fluxes in their spectral regions than do other sources, although any relative advantage is considerably less for photon flux than for brightness. If the feasibility of a contemplated experiment, time resolved or otherwise, is dominated by flux considerations, a wiggler may be the better source of synchrotron light.

2. The Advanced Light Source

The Advanced Light Source, a next-generation synchrotron source of XUV radiation, is under construction in Berkeley, California, at the Lawrence Berkeley Laboratory (LBL) of the University of California. The ALS is a U.S. Department of Energy-funded construction project with a total estimated cost of $99.5 million. Congress has already appropriated 93 percent of this amount, and the remainder is in the President's fiscal year 1992 budget. The

project is scheduled to be completed in April 1993. As a national user facility, the ALS will be available to visiting and in-house researchers from university, industrial, and federal laboratories.

As the highest priority project at LBL, the ALS is poised for success. LBL has a long history and extensive base of experience building and operating state-of-the-art accelerator facilities. An exceptionally strong and experienced team of scientists and engineers is dedicated to make the ALS succeed. LBL also has a demonstrated commitment and considerable experience operating national user facilities, such as the National Center for Electron Microscopy, which offers a broad array of imaging and analytical capabilities down to atomic length scales to a user community spanning many disciplines. In short, all the elements are in place for success.

The ALS facility consists of an accelerator complex, a complement of insertion devices, beamlines, and associated experimental apparatus, and a building to house this equipment. The state-of-the-art (low-emittance) storage ring has 10 straight sections available for insertion devices (undulators and wigglers). Initially, 24 high-quality bend-magnet ports will also be available. The undulators will generate high-brightness radiation at photon energies from below 10 eV to above 2 keV in the XUV region of the spectrum. The wigglers will access the hard x-ray region by generating broad-band radiation up to 20 keV. Bend magnets will be useful below 10 keV. Infrared radiation will also be available from the bend magnets. In the normal operating mode, the time structure of the radiation will comprise pulses with a full-width-half-maximum of about 30 ps and separation of 2 ns.

These capabilities will support an extensive research program in a broad spectrum of scientific and technological areas in which x-ray and ultraviolet radiation is used to study and manipulate matter in all its varied gaseous, liquid, and solid forms. New opportunities for research in materials, interface, and surface science, in atomic and molecular physics, in chemistry, in the life sciences, in earth science, and in x-ray optics will be available. The ALS will also serve those interested in developing the fabrication technology for micro- and nanostructures, as well as for characterizing them. In sum, the high brightness of the ALS will open new areas of research while the facility continues to serve as a reliable source for experimental techniques that have proven their worth in solving problems in basic research and applied technology.

3. Accelerator Overview

The ALS accelerator complex is described in considerable detail in a conceptual design report. An overall layout of the facility's accelerator complex, which consists of a 50-MeV linac, a 1-Hz, 1.5-GeV booster synchrotron, and an electron storage ring, is shown in Fig. 1. Table I lists the major parameters of the storage ring. Although the energy of the storage ring will range from 1 to 1.9 GeV, its performance is optimized at 1.5 GeV. Performance characteristics of the ALS are determined primarily by the design of the storage-ring magnet lattice. The ALS lattice has 12 long straight sections that are joined by 12 achromatic arcs, each containing three bend magnets. This structure is referred to as a triple-

bend achromat. Each of the 12 identical segments (superperiods) of the ALS lattice also contains six quadrupole focusing magnets and four sextupole magnets. The ALS lattice is optimized for the use of insertion devices. Of the 12 straight sections in the storage ring, one is used for injection and one is occupied by rf cavities, leaving 10 full straight sections available for undulators and wigglers up to 4.5 m in length. Each arc of the storage ring is fitted with four bend-magnet ports (Fig. 2). Of the maximum of 48 ports, 24 are so-called prime ports with superior properties and will be developed first.

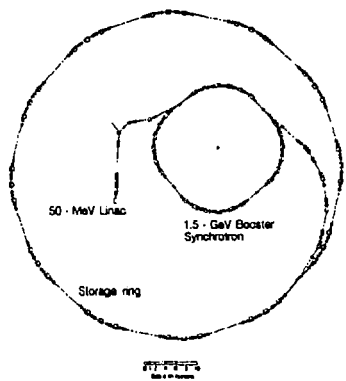

Fig. 1. Layout of the ALS accelerator complex showing the placement of the 50-MeV electron linear accelerator, the 1.5-GeV booster synchrotron, and the storage ring.

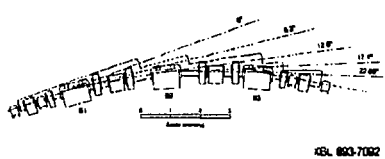

Fig. 2. Arrangement of photon-beam ports in one superperiod of the ALS storage-ring lattice showing an insertion-device port and four bend-magnet ports.

The ALS produces electron beams that are bunched rather than continuous. The storage-ring rf system has a frequency of 500 MHz, so the spatial separation between bunches is 0.6 m and the temporal separation is 2 ns. The storage-ring lattice, the rf system, and the

Table 1. Main Parameters of the ALS Storage Ring

Beam energy [GeV]	
Nominal	1.5
Minimum	1.0
Maximum	1.9
Circumference [m]	196.8
Beam current [mA]	
Multibunch	400
Single bunch	7.6
Beam emittance, rms [m·rad	
Horizontal	$<10^{-8}$
Vertical	$<10^{-9}$
Relative rms momentum spread	
Multibunch	8.0×10^{-4}
Single bunch	13.0×10^{-4}
Radiation loss per turn [keV]	91.5
Beam lifetime [h]	8
Nominal bunch duration, FWHM [ps]	30-50
Number of straight sections	12
Number available for insertion devices	10
Length for insertion devices [m]	4.5

impedance of the vacuum-chamber hardware determine the length (spatial and temporal) of the bunches. For the ALS at the nominal current of 400 mA, the predicted full-width-at-half-maximum (FWHM) value of the bunch length is 35 ps. Fig. 3 shows the electron-bunch structure. To avoid trapping positive ions in the potential well of the negatively charged electron beam, the multibunch mode with a 400-mA current will have 250 contiguous bunches, followed by a gap of 78 empty buckets. For particular experiments—for example, those involving time-of-flight measurements—it can be advantageous to have only one or a few circulating electron bunches in the storage ring. In the few-bunch mode, the nominal current per bunch will be 7.6 mA and the bunch length (FWHM) is predicted to be 55 ps, although still larger bunch currents may be tolerated (with additional bunch lengthening) before the beam becomes unstable.

4. Insertion Device Characteristics

The magnetic structure of an insertion device consists of a linear array of north-south dipoles of alternating polarity. The normal vertical orientation of the dipoles causes relativistic electrons of energy E to undergo a nearly sinusoidal electron trajectory of period λ_u in the horizontal plane, causing the emission of synchrotron radiation, as shown in Fig. 4. The peak magnetic field, B_0, on the undulator axis depends exponentially on the ratio R of the gap between the dipole north and south pole faces, g, to the period of the undulator, λ_u. For so-called hybrid devices made with the permanent magnet material neodymium-iron-boron, B_0, is approximately

$$B_0[\text{Tesla}] = 3.44\, e^{-R(5.47 - 1.8\, R)}$$

for $0.07 < R < 0.7$.

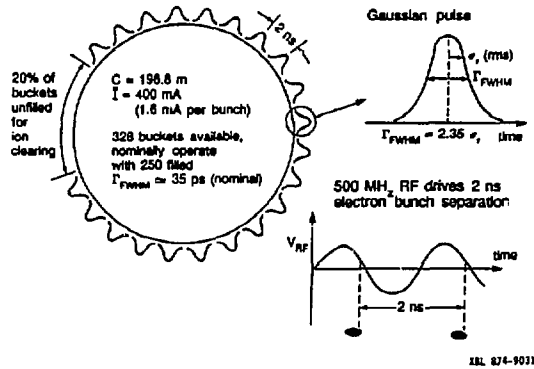

Fig. 3. Schematic illustration of the electron bunch structure in the ALS storage ring during multibunch operation. As shown at the upper right, each bunch has a full width at half maximum of about 35 ps. The spacing between bunches, dictated by the rf frequency, is 2 ns.

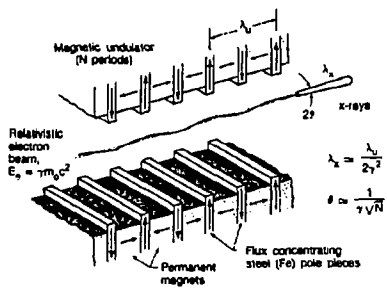

Fig. 4. Diagram of the magnetic structure of an undulator shows the main features of the hybrid technology that uses permanent-magnet material to drive steel pole pieces. North-south dipoles of alternating polarity bend electrons moving at nearly the speed of light into a sinusoidal trajectory, thereby causing the emission of a narrow cone of XUV radiation of high spectral brightness at a wavelength (λ_x) determined primarily by the electron-beam energy (E_e) and the undulator period (λ_u).

The deflection parameter K is the ratio of the maximum angular deviation of the electron trajectory from the insertion-device axis to the natural opening angle of the

synchrotron-radiation cone. The cone has a natural opening angle that is inversely proportional to the electron-beam energy. Expressed in terms of undulator parameters, K is approximately

$$K = 0.934\ B_0[\text{Tesla}]\ \lambda_u[\text{cm}].$$

Purists would say $K = 1$ defines the break point between an undulator and a wiggler. However, an insertion device retains significant undulator properties at higher K values, and most of the undulators planned for the new synchrotron sources operate in this intermediate range with $K > 1$. When $K >> 1$, the structure is called a wiggler.

In the undulator regime, an important effect comes into play that gives insertion devices special properties. Because of the rather gentle perturbation of the electron trajectory in an undulator (several micrometers amplitude), the electron trajectory during a pass through the device lies within one radiation-cone opening angle. This condition means that the radiation emitted from successive undulator periods add coherently. The interference behavior due to the coherence gives rise to a sharply peaked radiation spectrum consisting of a fundamental and several harmonics. The photon energy, ε_n, of the nth harmonic is

$$\varepsilon_n[\text{keV}] = \frac{0.949\ n E^2[\text{GeV}]}{\lambda_u[\text{cm}]}\left(\frac{1}{1 + K^2/2 + \gamma^2\theta^2}\right),$$

where γ is ratio of the electron relativistic and rest masses and θ is the angle of emission relative to the undulator axis. By contrast, the lack of interference in a wiggler means that its synchrotron radiation spectrum is like the broad, continuous spectrum from the dipole or bend magnets in the curved sections of the storage ring.

The angular dependence of the undulator photon energy give rise to a ring-like spatial pattern (Fig. 5), which has been vividly confirmed in photographs of rainbow rings at visible wavelengths produced by undulators in low-energy electron storage rings. As the angle increases, eventually the on-axis photon energy of, for example, the fundamental will reappear as the second harmonic of the off-axis fundamental. The angle for the mth ring of the same photon energy as the on-axis harmonic n is

$$\theta_{n,m} = \frac{1}{\gamma}\sqrt{\frac{m}{n}\left(1 + \frac{K^2}{2}\right)},$$

where $n+m$ is the ring harmonic.

It is important to the experimenter to be able to select the photon energy of the undulator light—that is, the light should be tunable. Providing this tunability is a challenge to undulator designers. In principle, the photon energy is tuned from high to low values primarily by decreasing the undulator gap g from a maximum to a minimum distance, thereby

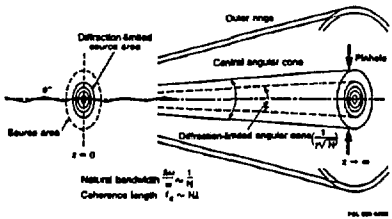

Fig. 5. Schematic illustration of the ringed radiation pattern from an undulator. A pinhole or other aperture can be used to select only the central cone of undulator radiation, thereby passing a sharply peaked spectrum centered around the on-axis fundamental and its harmonics.

increasing the field B_0 and the value of K. Both the minimum and the maximum are arbitrarily set by the drop off of the photon flux at low and high gap values, but are also subject to constraints such as the vertical diameter of the storage ring vacuum chamber. At the ALS, use of the third and fifth harmonics of the undulators is planned to extend their spectral range to higher photon energies than can be reached with the fundamental alone.

While tunable, undulators retain their most desirable properties in a comparatively small photon-energy range. For $K \ll 1$, the only significant photon flux is in the fundamental. As K is increased, the number of harmonics with measurable photon flux grows rapidly. It becomes useful to define a critical harmonic n_c above which half the total radiated power occurs. The critical harmonic is given by

$$n_c = 0.75K\left(1 + \frac{K^2}{2}\right).$$

The cubic dependence of n_c on K means that most of the undulator radiation is in the harmonics when tuning the undulator to lower photon energies (Fig. 6). These harmonics are spectrally broadened by electron-beam emittance and by the magnet errors discussed below and are not useful as high-brightness sources. But they are intense enough to require that substantial liquid cooling be used to avoid distortion or destruction of the first optical elements in the beamlines that guide the radiation from the storage ring to the experiment. Essentially, increasing K too far turns the undulator into a wiggler, as the higher harmonics blend together into a broad spectrum.

Many undulator properties improve with the number of periods N. For example, the intrinsic, on-axis spectral width (Full-Width-Half-Maximum) of the nth undulator harmonic is approximately

$$\Delta\varepsilon_n/\varepsilon_n = 0.9/nN\,.$$

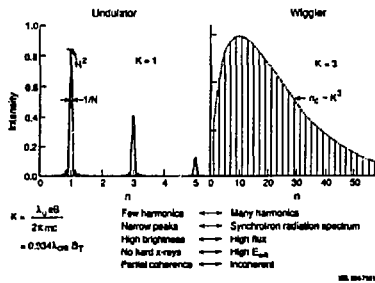

Fig. 6. The photon energies of the fundamental and harmonics of an undulator are conveniently tuned by varying the so-called deflection parameter, K, which is proportional to the peak magnetic field, B, and the undulator period, λ_u. But, as the magnetic field of the undulator increases, the device becomes more and more like a wiggler. The figure compares the properties of a undulator to those of a wiggler and shows how rapidly an undulator takes on wiggler properties.

In practice, the lower bound of the spectral width is limited by the angular divergence of the electron beam. Because electrons in the beam are not perfectly collimated, radiation observed on axis is actually emitted over a range of angles with a consequent spread in photon energies. When the intrinsic width drops below this spread, increasing the number of periods no longer improves the spectral resolution.

5. ALS Insertion Devices

Operating at 1.5 GeV, the ALS is optimized for insertion-device operation in the XUV spectral regions. Between them, the undulators will be able to excite the K shell of elements through silicon and the L shell of elements up to krypton, while the wiggler will be able to excite the L shell of nearly every element in the periodic table.

Table 2 lists the properties of three undulators (U8.0, U5.0, and U3.9, where the number refers to the period length in centimeters) that span the XUV spectral region when the ALS operates at 1.5 GeV. In addition, undulator U10.0, also included in Table 2, has been requested by a user group specifically to provide low-energy photons in the range 6-25 eV. The wiggler in Table 2 generates a broad continuous spectrum characterized by a critical photon energy ε_c, defined as the photon energy above which half the total power is radiated. At the high end of the broad wiggler spectrum, the flux drops rapidly but is still one-tenth of its maximum value at photon energies near $4\varepsilon_c$. With a wiggler ε_c of 3.1 keV, the ALS spectral range extends into the hard x-ray region above 10 keV. High-quality synchrotron radiation will be available from the 24 prime bend-magnet ports as well. The critical photon energy of the bend magnets is 1.56 keV.

Table 2. Parameters for initial ALS insertion devices

Name	Period [cm]	No. of periods	Photon energy range [eV] [a]	Critical energy [keV]
Undulators				
U10.0	10.0	45	— [b]	—
U8.0	8.0	55	5.4–220 [c] [16.2–660] [27–1100]	—
U5.0	5.0	89	52–380 [156–1140] [260–1900]	—
U3.9	3.9	115	169–500 [507–1500] [845–2500]	—
Wiggler				
W16	16	16	—	3.1

[a] The photon energy range of the fundamental and of the third and fifth harmonics (shown in brackets) as the deflection parameter K decreases from its maximum value to approximately 0.5, when the electron-beam energy is 1.5 GeV.
[b] Only the range from 6 to 25 eV in the fundamental will be used.
[c] Below about 8 eV in the fundamental, the peak field in undulator U8.0 exceeds the bend-magnet field and may adversely affect storage-ring operation.

Engineering designs are well under way for the initial complement of insertion devices. The design philosophy is to create a generic design, as shown in Fig. 7, and thereby reduce engineering and fabrication costs and enhance maintainability. The goals of very high brightness and useful fifth-harmonic output impose unusually tight tolerances on the magnetic-field quality and thus on the mechanical structure of the undulators. The ideal undulator is designed to be as nearly transparent to the electron beam as possible; that is, the beam emerging from the downstream end should be the same as if there were no undulator at all. Transparency is never fully achieved, and real undulators may have bending, focusing, and other effects on the electron beam. At the ALS, however, accelerator physicists have made detailed numerical simulations of the effects of undulators and wigglers on the stored beam that demonstrate that, while there is a significant effect, it is only slightly greater that those expected from random magnetic-field errors in the storage-ring magnets.

To minimize effects on the stored electron beam due to undulators, as well as wigglers, it is necessary to put severe limits on the allowed net dipole, quadrupole, and other components of the magnetic field over the length of an undulator. These limits in turn place equally severe restrictions or random magnetic field errors. The cumulative effects of these

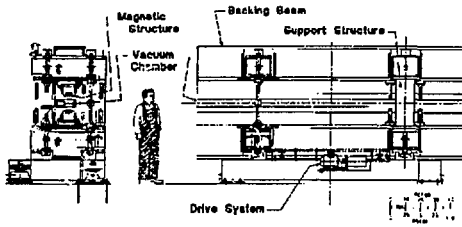

Fig. 7. Drawing of a generic insertion device for the straight sections of the ALS storage ring showing the main structural features that all undulators and wigglers will have in common. Undulators will be about 4.5 meters in length. The figure of the engineer give a sense of scale for the structure needed to precisely maintain and manipulate the undulator's magnetic structure in the face of large magnetic forces.

random errors can also significantly degrade the brightness of undulator radiation. Random field errors cause a loss of phase coherence that spectrally broadens the undulator harmonics, so that the brightness in a given spectral interval (the spectral brightness) drops. Moreover, systematic errors, such as a continuous change in the amplitude of the sinusoidal magnetic field over the length of the undulator, reduce the brightness because the spectrum of the undulator radiation shifts from one part of the device to the next (the spectrum chirps).

In general, the use of high harmonics from undulators with many periods in a low-energy ring obliges the engineer to take the most care to minimize field errors. The ALS fits into all three categories. Taking all error sources into account, physicists have arrived at a magnetic-field rms error budget that allows for a net error of 0.25% for undulator U5.0, which is just at the state of the art. The error budget for U8.0 is slightly more relaxed.

6. Spectral Brightness and Coherence

In a storage ring with electron current I, the total power P_{tot} radiated by an undulator of length L over all harmonics and angles is

$$P_{tot}[\text{kW}] = 0.633 E^2[\text{GeV}] B_0^2[\text{Tesla}] I[\text{Amp}] L[\text{m}].$$

For many purposes, it is only the central cone of undulator radiation that experimenters use. The spectral flux F_n or flux per unit bandwidth, BW, for the nth harmonic integrated over the cone is

$$F_n[\text{photons/sec/0.1\% BW}] = 1.43 \times 10^{14} I[\text{Amp}] N Q_n(K),$$

where Q_n is a function of value less than or equal to 1 that increases with K and decreases with n. The flux increases linearly with N

The spectral brightness is the spectral flux per unit area of the source and unit solid angle of the radiation cone. In the jargon of statistical mechanics, the brightness is the density of flux in phase space. The average spectral brightness B_n in the central cone is approximately

$$B_n[\text{photons/sec/mm}^2\text{/mrad}^2\text{/0.1\%BW}] = \frac{F_n}{(2\pi)^2\Sigma_x\Sigma_{x'}\Sigma_y\Sigma_{y'}} = \frac{3.62 \times 10^{12}\, I[\text{Amp}]NQ_n(K)}{\Sigma_x\Sigma_{x'}\Sigma_y\Sigma_{y'}},$$

where Σ_x and Σ_y are the rms source sizes in x and y coordinates for a beam with a Gaussian density distribution, and $\Sigma_{x'}$ and $\Sigma_{y'}$ are the rms cone opening angles (angular divergence). The source size is obtained by adding in quadrature the size of the electron beam and the source size of a diffraction-limited photon beam. The angular divergence is obtained in an analogous manner. In most cases, the brightness varies linearly with N. Brightness is a conserved quantity that cannot be improved by an optical system; it therefore represents a true source characteristic. Absorption, scattering, and poor design can, of course, degrade the brightness downstream from the synchrotron source.

The critical harmonic of a low-K undulator lies at lower photon energies than the critical energy of the same device operated as a high-K wiggler. But, when the radiation is concentrated in a few harmonics, these become much brighter (up to several hundred times) than slices of the same spectral width from a wiggler. As a bonus, in so-called planar undulators, the radiation in the plane of the electron orbit turns out to be highly linearly polarized with the electric field vector in the orbit plane. Spectral brightness is shown in Fig. 8 for the undulators and wiggler described in Table 2, the ALS bend magnets, and for representative sources at other facilities. The spectral brightness of ALS undulators is shown in more detail in Fig. 9 for the fundamental and the third and fifth harmonics of the undulators.

A significant fraction of the radiation from the ALS undulators is spatially coherent. The criterion for spatial coherence is that the product of the area of the light source and the solid angle into which it emits be no larger than the square of the wavelength of the light. Since this is the diffraction condition, spatially coherent light is also said to be diffraction-limited. In accordance with the diffraction condition, the electron-beam emittance e sets the minimum wavelength at which all the radiation can be diffraction limited, according to the relation

$$\epsilon = \lambda_{min}/4\pi.$$

Even at wavelengths below the minimum, part of the radiation remains diffraction limited, the fraction decreasing as the square of the wavelength. In addition, for practical optical systems, it is possible to use several radiation modes without significantly losing resolution (Fig. 10), thereby increasing the effective fraction of coherent radiation.

Although phase-sensitive techniques, such as holography, most naturally come to mind when thinking about coherent radiation, a more general virtue is the ability to focus. For

example, a Fresnel zone plate can focus a coherent beam of soft x-rays to a spot whose radius is approximately 1.2 times the width of the outermost zone. With state-of-the-art microfabrication techniques, such as electron-beam lithography, it is possible to make zone plates with outer zone widths of about 300 Å. This capability can be exploited in scanning systems in which the focused x-ray beam sweeps across a sample to generate imaging or spatially resolved spectroscopic information with a comparable resolution.

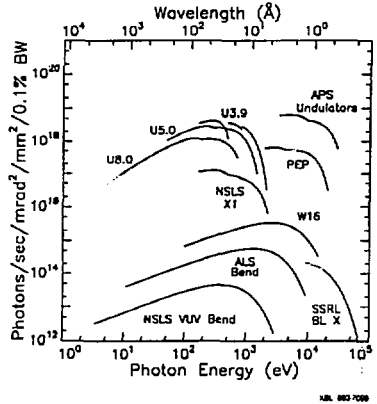

Fig. 8. With the use of more than one undulator harmonic it is possible to cover a wide spectral range. The spectral brightness envelopes are shown for the three ALS undulators and wiggler described in Table 2, the ALS bend magnets, undulators planned for the Advanced Photon Source (APS), and representative insertion-device and bend-magnet sources at the National Synchrotron Light Source (NSLS) and the Stanford Synchrotron Radiation Center (SSRL). X-1 is a recently installed undulator beamline at NSLS. The discontinuities in the undulator curves represent a shift from the envelope of the fundamental to that of the third harmonic, etc. The spectral brightness of the undulators greatly exceeds that of other sources shown in the drawing.

7. Insertion-Device Beamlines

Low-emittance storage rings and insertion devices have created new challenges for designers of XUV optics. First, the source size and divergence have become smaller. For ALS undulators at the high-photon-energy end of the spectral range, the rms size is typically 330 μm horizontal by 65 μm vertical and the rms divergence is typically 40 μrad horizontal by 30 μrad vertical. The smaller source size requires tighter tolerances for relay optics and monochromator components in both optical figure and finish to avoid loss of light (e.g., rms

surface roughness ≈ 0.5 nm and tangential slope error <1 μrad for a condensing mirror). The attainment of higher resolution by use of smaller slits also becomes practical (the spectral-resolution goal of monochromators in undulator beamlines is $\Delta E/E \approx 10^{-4}$). Monochromator components therefore need tighter tolerances to avoid loss of resolution. Finally, the photon-beam power has increased to several kw/cm². The requirement that thermal distortions and stress be controlled complicates the design [for example, water cooling in a UHV (≈ 1 ntorr) environment is required] and limits the choice of materials.

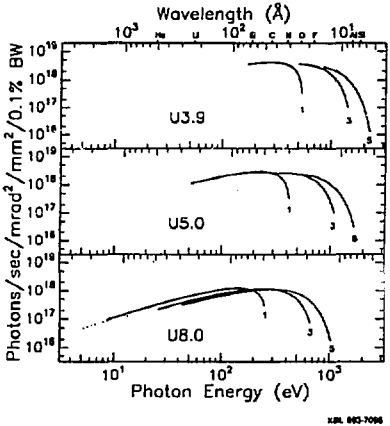

Fig. 9. Spectral brightness as a function of photon energy for the three undulators described in Table 2. Each undulator curve is the locus of narrow peaks of radiation, tuned by altering the undulator gap. Separate curves are shown for the fundamental and the third and fifth harmonics of each undulator. The dotted extension of the fundamental of U8.0 represents the theoretical performance at large values of the deflection parameter K. Undulator U10.0 will be used to cover this spectral range.

The most serious limitation is that of optical fabrication tolerances. It is difficult to fabricate aspheric optical surfaces (paraboloids, ellipsoids, toroids, etc.) sufficiently accurately in mirrors, monochromators, and other optical elements to take full advantage of the undulator source. One way to address this problem is to avoid the use of aspheric surfaces and to build beamlines entirely with plane and spherical surfaces. Although studies at LBL and elsewhere have confirmed that, when a large heat load is present, thermal considerations dominate the design and cost of the beamline, undulators usually generate lower total power

than wigglers For the ALS undulator beamlines, the power problem is significant but within the state of the art.

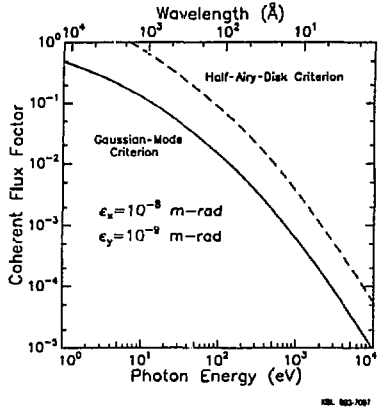

Fig. 10. Fraction of the flux from ALS undulators that is transversely coherent according to two criteria. From statistical optics, the fraction of coherent flux in a single Gaussian mode is a dimensionless ratio involving only the photon energy, the electron-beam emittance, and the undulator length. For practical optical systems, its is possible to use several radiation modes without significantly losing spectral resolution, as reflected in the half-Airy-disk criterion.

To meet these challenges, the initial ALS-constructed undulator beamlines are based on the spherical-grating monochromator system with water-cooling. The strategy is to use spherical surfaces for all mirrors and gratings and to actively water-cool the optics. Depending on the beamline requirements, the condensing system chosen for ALS undulator beamlines consists of one or two spherical mirrors. (Users are free to choose other optical designs for beamlines that they construct, subject to approval by the ALS.) Because of the low emittance of the ALS storage ring, the monochromator can accept the entire undulator beam in most cases, even at a slit-width of 10 μm.

Engineering design of the ALS-constructed beamlines is now under way, with numerous changes occurring as individual problems are encountered and solved. The undulator beamlines, comprising a front end inside the storage-ring shielding wall and a branchline outside the wall, that are actually constructed may differ in some ways from the following descriptions.

Figure 11 shows the beamline layout for the U5.0 beamline front end (top) and

branchline (bottom). The front end components, with the exception of the photon beam-position monitor, are primarily for protection of the beamline equipment, the storage-ring vacuum, and, most important, personnel. The photon shutter is water cooled. The beam-position monitors provide information to a feedback system that will locate and stabilize the position and angle of the electron beam at the center of the undulator to 10 percent of its rms size and divergence.

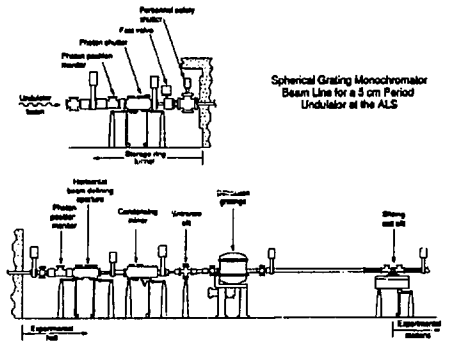

Fig. 11. Beamline layout for the U5.0 beamline. The front end inside the storage-ring shield wall is shown on the top; the branchline outside the storage-ring shield wall is shown on the bottom. User-supplied optics beyond the monochromator and the experimental stations are not shown.

The branchline includes a spherical-grating monochromator with three water-cooled diffraction gratings that can cover the range of photon energies from 65 eV to 1500 eV. When the undulator gap is at a minimum (maximum K), as discussed earlier, photons will be generated in large numbers from harmonics higher than the fifth and at photon energies higher than 1500 eV. The primary branch is designed to deliver photons from the fundamental and the third and fifth harmonics with minimum losses and high spectral resolution. The water-cooled beam-defining aperture passes the entire central cone of undulator radiation. The condensing mirror, also water-cooled, focuses a vertical image of the source, demagnified by a factor of about 15, onto the monochromator entrance slit. The grating images the entrance slit onto an exit slit that moves in such a way that the image remains in focus as the grating rotates. The Rowland circle condition is satisfied at only two wavelengths, but third-order aberrations are small enough so that the resolution remains determined by the size of the entrance slit. To focus the source image onto the sample, refocusing optics after the monochromator exit slit are required and depend on the specific application for which the

beamline is intended. The pressure in the beamline must be less than 0.5 ntorr.

Figure 12 shows the beamline layout for the U8.0 beamline front end (top) and branchline (bottom). The branchline includes a spherical-grating monochromator with three water-cooled diffraction gratings that can cover the range of photon energies from 20 eV to 300 eV. Apart from the photon-energy ranges covered, there are two main differences between the U5.0 and U8.0 branchlines. The first is that, in addition to the primary U8.0 branchline, deflection mirrors could be introduced to generate secondary branches that would bypass the monochromator. This opportunity arises from the larger angles of incidence possible for mirrors at lower photon energies. The second difference is that a horizontal focusing mirror is the first optic in the U8.0 branchline. Horizontal focusing before the monochromator is required when operating the undulator at large values of K because the divergence of the undulator beam increases in the horizontal direction under these conditions. Moreover, the beam power is highest at large K and the horizontal mirror can absorb power as the first optic without affecting beamline performance.

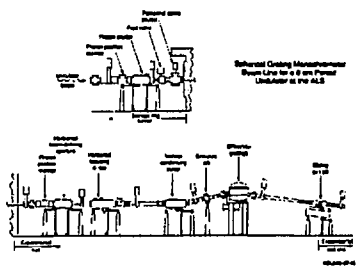

Fig. 12. Beamline layout for the U8.0 beamline. The front end inside the storage-ring shield wall is shown on the top; the branchline outside the storage-ring shield wall is shown on the bottom. User-supplied optics beyond the monochromator and the experimental stations are not shown.

8. Scientific Program

The initial scientific program emphasizes the high brightness of XUV light available from the ALS. The program is being implemented by means of participating research teams (PRTs) consisting of investigators with related research interests from one or more institutions. The primary responsibility for experimental apparatus rests with the PRTs; the responsibility for the beamlines and, where appropriate, insertion devices will be shared between the ALS and the PRTs. In return for its commitment, each PRT receives a guaranteed fraction of the ALS operating time at its beamline. A substantial fraction of the ALS running time at each beamline will also be made available to independent investigators not affiliated with a PRT by means of a proposal process.

PRTs working with undulator or wiggler beamlines are called insertion-device teams. Other PRTs work with bend-magnet beamlines and are known as bend-magnet teams. A Call for Proposals issued in the spring of 1989 resulted in 18 proposals from both insertion-device and bend-magnet teams. Nine insertion-device teams, which subsequently coalesced into the eight that are listed in Table 3, were approved in December 1989. Figure 13 shows a layout of the ALS building with possible locations of insertion devices and associated beamlines. Four bend-magnet teams that were approved in June 1990 are listed in Table 4. Including three additional ports allocated to insertion-device teams, seven of the 24 available prime bend-magnet ports have been spoken for. More than 200 persons, mostly from universities and federal laboratories, participated in the first round of PRT proposals.

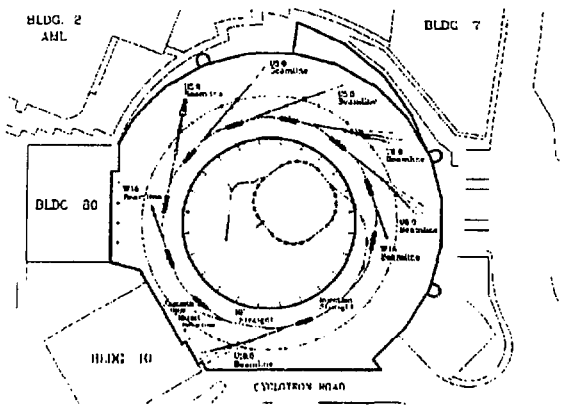

Fig. 13. Floor plan showing a possible placement of insertion devices and locations of associated beamlines in the ALS building. The maximum beamline length is about 35 m. The prime bend-magnet ports to be developed initially are located in the center bend magnet of each storage-ring arc. At two ports per magnet, there is a total of 24 ports.

Some of these groups are expected to use the high brightness of the ALS undulators to open new areas of research in the materials sciences, such as spatially resolved photon and electron spectroscopy (spectromicroscopy). Biological applications will include x-ray microscopy with element-specific sensitivity in the water window of the spectrum (23-44 Å) where water is much more transparent than protein, thereby allowing soft x-rays to penetrate the natural aqueous environment of these systems. The ALS will also be an excellent research

tool for atomic physics and chemistry because the high flux will allow measurements to be made with tenuous gas-phase targets. The short pulse width (30-50 ps) will facilitate time-resolved experiments. A future option is the construction of special devices to generate radiation with a controlled elliptical polarization.

Table 3. Insertion-Device Participating Research Teams (PRTs)

Insertion Device	Scientific Focus	Spokesperson
U10.0	Chemical dynamics	Tomas Baer U. of North Carolina
U8.0	Atoms, molecules, ions	Denise Caldwell U. of Central Florida
U8.0	Pump-probe, timing, dynamics experiments	R. Stanley Williams U. of California, Los Angeles
U5.0	Surfaces and interfaces	Brian Tonner U. of Wisconsin-Milwaukee
U5.0	Surfaces and interfaces	Joachim Stöhr IBM Almaden Research Center
U3.9	X-ray imaging and optics for the life and physical sciences	Stephen Rothman U. of California, San Francisco
W16	Atomic, molecular, optical physics; materials science	Bernd Crasemann, U. of Oregon Philip Ross, LBL
W16	Life sciences	Stephen Cramer, U. of California, Davis

Major research areas proposed for ALS undulator beamlines include: (1) soft x-ray microscopy of materials, surfaces, and biological systems, (2) spatially resolved spectroscopy (spectromicroscopy) of materials, surfaces, and biological systems, (3) high-resolution soft x-ray spectroscopy of materials and surfaces, (4) soft x-ray gas-phase spectroscopy of atoms and molecules, (5) molecular spectroscopy and dynamics with synchrotron radiation/laser pump-probe methods (6) spin-polarized photoemission spectroscopy. and (7) polarization-dependent experiments, such as circular dichroism of biological systems.

Wiggler-based x-ray studies will include spectroscopy of atoms in both the gas phase and in condensed matter, spatially-resolved elemental analysis with an x-ray microprobe, grazing-incidence x-ray scattering from surfaces, and x-ray diffraction of large biological molecules (protein crystallography). Bend-magnet research will include studies of physical and biological systems with polarized radiation and infrared absorption spectroscopy of solids, surfaces and gases.

Table 4. Bend-Magnet Participating Research Teams (PRTs)

Scientific Focus	Spokesperson
Soft x-ray spectroscopy and time-resolved studies of materials and surfaces; x-ray optics	James H. Underwood Lawrence Berkeley Laboratory
EUV spectroscopy and time-resolved studies of materials, surfaces, and gases; x-ray optics	James H. Underwood Lawrence Berkeley Laboratory
Infrared spectroscopy and time-resolved studies of surfaces, solids, and gases; fast IR detectors	Gwyn P. Williams Brookhaven National Laboratory
Polarized photon studies: accelerator and beam diagnostics, spin-dependent interactions of photons with matter, chiral biological molecules	Mervyn Wong Lawrence Berkeley Laboratory

9. Atomic and Molecular Physics

An outstanding feature of the ALS will be its high brightness, which will result in increased intensity on the target relative to less bright sources for two kinds of experiments:

- Experiments with tenuous targets which occupy a small volume (e.g., when the target is a focused beam of ions), or experiments where only those interactions which take place in a small volume are of interest, (e.g., focusing the x rays into the entrance volume of an electron analyzer);
- High-resolution experiments, where the high brightness serves to allow focusing all of the x-ray beam onto the entrance slit of a monochromator.

The ALS will therefore be useful for a variety of experiments in atomic and molecular physics and materials science, where the tenuous target might be an atomic vapor, laser-excited atoms or molecules, an ion beam, ions in a trap, clusters, or actinides (which might be too radioactive or too rare to permit a large target). The high resolution will be useful for experiments with atoms or molecules (e.g., looking at doubly excited states of atoms or vibrational structure of molecules).

Another class of applications of high brightness consists of coincidence experiments, where more than one reaction product must be detected simultaneously; a very intense x-ray beam is required to generate a large enough signal to compensate for the limited solid angle or low efficiency for detecting one or both products.

The short pulse length of the ALS will be useful for a variety of experiments in chemistry, in which two or more photons are used to study a system (often called two color or multi-color experiments, or pump-probe experiments). As applied at the ALS, one photon will typically be a VUV photon or x ray from an undulator, and the second photon could be from an adjacent bend magnet or from an auxiliary laser.

An active research program in most of these areas is planned; please contact the authors for additional information regarding access to the ALS.